We thank the reviewer for her/his time and comments, which are reproduced in *black italic font* below. Our responses are shown in regular font. Revised text (as it appears in the manuscript) is shown in blue font. Line numbers are those of the revised manuscript with changes accepted.

Anonymous Referee #1 Received and published: 5 June 2020

This paper discusses the optimization of a HONO calibration source suitable for field work. For many instruments, the source needs to be relatively free of compounds that could interfere with the measurements of HONO. Current methods of HONO production often produce concentrations that vary with operating conditions (humidity, temperature, flow rates), as well as requiring long periods before stable outputs are achieved. Because of issues of stability and reproducibility, the output of HONO calibration methods need to be confirmed in the field with a secondary HONO instrument, often an absolute measurement technique such as absorbance spectroscopy or a chemiluminescent NOx analyzer. Ideally, a field calibration source would provide stable and reproducible concentrations of HONO that could be quantified in the laboratory and reliably reproduced in the field, such that a secondary instrument would not be needed for source quantification.
The source described in this paper is based on the design of Febo et al. (1995), which has been used extensively by other groups as outlined in the manuscript. The authors describe changes in the design of the source that appear to minimize impurities such as ClNO and NOx, and characterize the output of the source using FTIR and TDCRDS instruments. They find that their "optimized source" can produce concentrations of HONO with approximately 97% purity and is stable after 1.5 hours. The authors report HONO concentrations from the source ranging between 1.5 and 3 ppm from FTIR experiments and 11 and 50 ppb from TD-CRDS experiments (with some dilution occurring). The paper does provide some new information regarding the production of a stable, high purity HONO source for instrument calibrations and is likely of interest to the atmospheric chemistry community. While worthy of eventual publication, the paper does not provide sufficient information to give the reader confidence in reproducing the measurements. More experimental details regarding the individual flow rates, humidity, and temperatures should be provided. It is also not clear whether the source routinely produces concentrations of HONO with the stated purity over a range of operating conditions. The authors should include measurements of the HONO concentrations and impurities produced by the source over a range of temperatures and humidities that may be encountered when the source is used in the field. The authors should also provide information on the reproducibility of the source using the same operating conditions after it has been turn off. Illustrating that the output of the source is stable and reproducible from day-to-day might suggest that the source could be robust enough to be used for instrument calibrations without requiring a secondary instrument for quantification in the field.

Response: We appreciate the reviewer's point of view and agree that the manuscript would be strengthened by including a summary of our results with the optimized source in both the lab and the field.

We added the following on line 152 (to the materials and methods section):

"2.4 Field deployment
The HONO source was utilized during the "Study of nitrogen oxides in winter downwind from oil and gas sands" (SNOWDOGS) field campaign in Fort McKay, Alberta, Canada, in January 2020. Its output was quantified in parallel by TD-CRDS and a Thermo 42i-Y NO-NO$_y$ CL instrument equipped

with a Mo converter heated to 325 °C. This converter and the TD-CRDS quartz inlets were mounted on the roof of a trailer which housed the instruments and the HONO source. The TD-CRDS sampled at a flow rate of ~1.2 slpm per channel through ~5 cm short, 300 μm i.d. stainless steel flow restrictors placed inline after the heated quartz sections and before the Teflon filter assembly. The HONO source output was delivered via a 5 m long, 1/4" (0.64 cm) o.d. and 3/16" (0.48 cm) i.d. FEP Teflon tube to both instruments."

We expanded the text on line 232:

"**3.3 Source stability**
The source output gradually decreased over a time scale of weeks of continuous use, which was rationalized by the visible depletion of the HCl permeation tube. However, the source output remained stable and reproducible on shorter time scales. An example FTIR time series is shown in Figure 5, which was acquired after 1 month of intermittent use. After a 1.5 hours stabilization period, the source produced a stable output of 1.57 ppmv of HONO (from >1.0 ppmv of HCl) with a precision of ±35 ppbv.

3.4 Source purity and day-to-day reproducibility

The optimized source routinely delivered HONO in high purity (range 96.0% - 98.7%), as long as scrubbed, moisture-containing room air was used as diluent gas (Table 2). When dry cylinder gas was used instead, the source output was stable but contained a larger amount of undesired side products; for example, on July 25, 2019, the output contained 4.6% NO_2 and 8.8% NO + ClNO (Table 2). When used in the field, the performance was similar: with scrubbed air, the HONO purity was 98.5%, whereas with dry cylinder gas, the purity was merely 81.3% (Table 2 and Figure S5)."
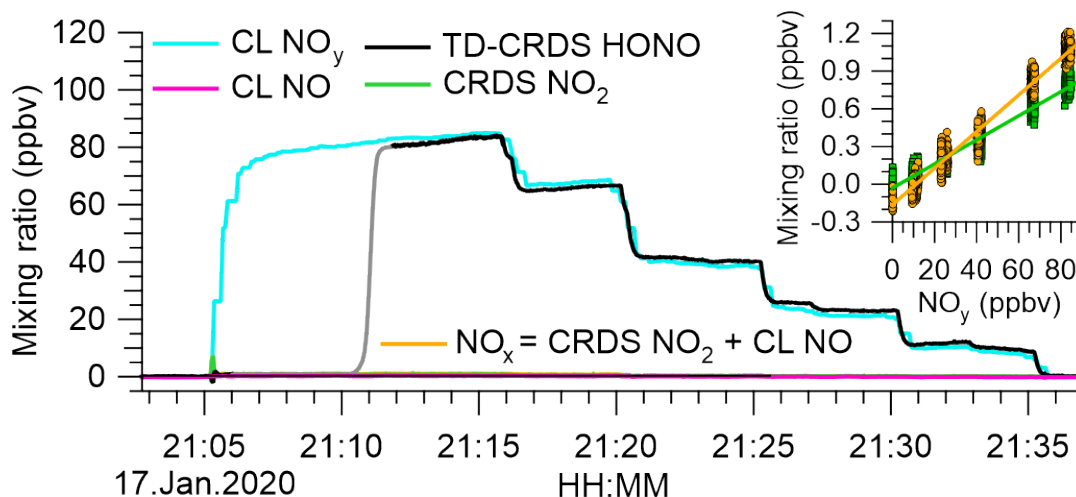
We added Table 2, which summaries our analysis results, on line 414:

"**Table 2.** Summary of TD-CRDS analyses of the HONO source output. The RH of the diluent gas was in the range of 15% to 35%, except for experiments conducted with cylinder gases which are shown below the dashed line. The range of mixing ratios stated is for output after dilution. The stated errors are from regression analyses of plots of NO_2, NO_x or NO_x+ClNO vs. NO_y and are at the 1σ level. n/d = not determined.

Date	Setting	Diluent gas	Range (ppbv)	HONO (%)	NO_2 (%)	NO_x (%)	NO_x+ClNO (%)
Jan 16, 2019	Lab	Scrubbed air	0 - 140	*97.2±0.1	n/d	2.80±0.07	n/d
May 3, 2019	Lab	Scrubbed air	0 - 7	96.0±0.2	1.9±0.2	4.0±0.2	(4.0±0.2)**
May 6, 2019	Lab	Scrubbed air	0 - 93	96.4±0.4	1.9±0.4	3.6±0.4	(3.6±0.4)**
May 10, 2019	Lab	Scrubbed air	0 - 21	*97.6±0.1	1.10±0.03	2.40±0.05	n/d
May 17, 2019	Lab	Scrubbed air	0 - 38	98.7±0.1	0.01±0.02	0.92±0.01	1.25±0.01
May 22, 2019	Lab	Scrubbed air	0 - 14	97.7±0.1	1.29±0.06	1.54±0.06	2.28±0.04
Jan 17, 2020	Field	Scrubbed air	0 - 80	98.5±0.1	1.00±0.05	1.50±0.08	(1.50±0.08)**
Mar 19, 2020	Lab	Scrubbed air	0 - 320	*98.72±0.01	n/d	1.28±0.01	n/d
Jul 25, 2019	Lab	Cylinder O_2	0 - 95	86.60±0.02	4.60±0.03	n/d	13.4±0.02
Jan 30, 2020	Field	Cylinder N_2	0 - 50	81.3±0.1	5.90±0.09	n/d	18.7±0.1

To the SI, we added

"**Figure S5.** Sample field analysis of the HONO source output. The TD-CRDS and CL instruments sampled scrubbed "zero" air before 21:05 and after 21:36. The HONO source output was added at 21:05:30. Only the CL NO_y responded because the TD-CRDS quartz inlet temperature was 200 °C. At 21:10, the temperature of the quartz inlet was increased from 200 °C to 600 °C to quantify HONO. The absence of an inflection point and prior agreement with the NO_x measurement implies the absence of ClNO. At 21:16 and every ~5 min thereafter, the HONO output concentration was decreased by slightly opening the bypass valve. The insert shows scatter plots of NO_2 and NO_x (calculated by adding CL NO and CRDS NO_2 data) against NO_y. Slopes and offsets were (0.96 ± 0.05)% and $-(30\pm3)$ pptv for NO_2 (points shown in green) and (1.46 ± 0.08)% and $-(164\pm4)$ pptv for NO_x (data points shown in orange), respectively."

Finally, we revised the statement given in the abstract on line 15:

"The source produces gas streams containing HONO in air in > 95% ~~97%~~ purity relative to other nitrogen oxides." to account for the observation of (96 ± 0.2)% purity on May 3, 2019 (Table 2).

Specific comments:

Methods: As mentioned in the paper, previous studies have demonstrated that the production of HONO by reaction R4 requires the gas stream to be humidified. However, the authors do not state the humidity of the gas stream used in their experiments.

Response: We added the following on line 88: "For the experiments shown in this manuscript, the relative humidity of the diluent gas stream was in the range of 15% to 35%. "

Page 4, line 88: Is there any reason for the 20 ccm dilution with O2?

Response: The additional flow is probably not essential, but we found it practical to keep part of the setup under flow of a clean gas - our laboratory air contains surprisingly high levels of NO_x delivered from the building's air intake, plus the continued flow would remove any impurities that might build up. The use of a second mass flow controller was also advantageous as it allowed the residence time and HCl concentration to be changed on the fly without disturbing the permeation tube setup (which can take quite a long time to return to a stable output when flows are changed).

We modified the text on line 90 as follows:

"The permeation tube was placed inside a glass chamber (VICI Dynacalibrator Model 120) whose temperature was controlled at 25.0 °C and which was continuously flushed at a flow rate of ~0.15 L min^{-1} with room air scrubbed using activated charcoal for a period of several days into a fume hood. The use of scrubbed air ensured that the gas stream contained water to maintain efficient HONO production (Schiller et al., 2001).

The HCl output was diluted in a gas stream of O_2 (~20 mL min^{-1}); this gas stream also served to continuously flush the connecting tubing when not in use."

If so, why O2 and not N2, zero air, or scrubbed room air?

Response: The reviewer is correct that either N_2, zero air or scrubber air could have been used. We chose O_2 because an O_2 cylinder was already in place for the O_3 generator. No changes were made.

Page 4, last paragraph: How much dilution was typical? What are final flow rates? More experimental details should be provided.

Response: We diluted the output by factors between 5 and 200, depending on how much HONO we desired to deliver on any particular day at a flow rate marginally larger than the TD-CRDS inlet sample flow. We modified the paragraph as follows:

"To deliver HONO in atmospheric concentrations (i.e., < 10 ppbv), a portion of the source output was directed towards waste with the aid of a pump and a needle valve. The output concentration could be rapidly changed (typically by factors between 5 to 200) by adjusting the position of the needle valve. The remaining output was diluted using scrubbed air and directed towards the instruments at a final flow rate slightly larger than the sampling requirement of the instruments. "

Fig. 1: The position of the needle valve and dilution do not match the written description. The figure only shows the input of the TD-CRDS being diluted and not the FTIR, while the text describes dilution before both instruments.

Response: As stated on line 107, the needle valve was used to deliver HONO in atmospheric concentrations (i.e., < 10 ppbv). The FTIR sampled the output without dilution, and the Figure is accurate as shown. We clarified this on line 111:

"Gas streams exiting the HONO sources (prior to dilution) were analysed using an FTIR spectrometer"

The schematic would benefit with typical flow rates.

Response: This information has been added to Figure 1.

Page 7, line 161: In this discussion, the authors are probably referring to reaction R5, and not R6.

Response: We thank the reviewer for catching this error. It has been corrected (line 177). We also corrected another error of this type on line 165.

Page 7, line 169: It appears that the improvement in source 2 is only a reduction of ClNO contamination, as both the NO and NO2 concentrations increased. This should be clarified.

Response: The reviewer's observation is correct. The issue with both source 1 and source 2 was that there was too much HONO produced, which can generate side products by either R-1 or R5. In source 2, more HONO was produced than in source 1 (because the rate of R5 was reduced) which increased the rate of NO and NO_2 produced via R-1.

We added the following on line 185: "... an improvement over source 1 in terms of unwanted ClNO production but still inadequate."

Page 8, equation 2: Check the equation – there appears to be an error translating the fonts.

Response: Apologies - this was an error converting word (.docx) to pdf format. Equation (2) is

$$[\text{Observed}]_{\text{total}} = [NO_x] + [ClNO]\left(1 - e^{-A_{ClNO} \times e^{\frac{-E_{A,ClNO}}{RT}} \times t_{res}}\right) + [HONO]\left(1 - e^{-A_{HONO} \times e^{\frac{-E_{A,HONO}}{RT}} \times t_{res}}\right)$$

This has been corrected in the revised document.

Fig. 5: The authors should define the lighter shaded points in both plots. Are the lighter shades indicating points while the source is stabilizing? If so, why are there lighter shade points at the end of the time series?

Response: Our apologies - the two lighter shade points at the end of the time series should have been in dark shade as well; this has been corrected. We also modified the caption as requested.

"Figure 5. Time series of HONO and HCl mixing ratios derived from FTIR analysis of the undiluted HONO source output. The NaNO$_2$ was placed in line at 10:10. Data acquired during the initial period are shown in light grey colour. The shaded areas represent the average $\pm$ 2σ after the source output had stabilized (after 11:45; data points shown in black colour). The 1σ precision of the HONO data was $\pm$35 ppbv and that of the HCl data was $\pm$42 ppbv. The HCl mixing ratios are an underestimate because the widths of their absorption lines are less than the FTIR's resolution of 0.5 cm^{-1}."

The authors should clarify how they determined that the output had stabilized.

Response: In the caption of Figure 5, we had stated "The shaded areas represent the average $\pm$ 2σ after the source output had stabilized (after 11:45; data points shown in black colour)."

Since we didn't apply a mathematically rigorous criterion to determine output stability, we changed the above to:

"The shaded areas represent the average $\pm$ 2σ after the source output ~~had~~ was judged to have stabilized (after 11:45; data points shown in black colour)."

We had judged whether the output was stable (or not) by visual inspection but also had performed a few simple statistical tests for corroboration.

A stable output is achieved when the output mixing ratio is not changing. For the data shown in black, this criterion is met since the slope of a linear regression fit is -(0.4$\pm$1.9)$\times$10^{-6} s^{-1} $\approx$ 0.

We also calculated the average (μ) and standard deviation (σ) for this period which were 1.596 and $\pm$0.036 ppmv. The residuals during this time period were normally distributed (i.e., reproduced by a Gaussian equation, see figure below).

The μ$\pm$2σ interval is shown as a grey area in Figure 5; since the noise is normally distributed, this interval is expected to encompass 95% of the data; for the data shown in black, 6 of the 132 (~4.5%) are outside this confidence interval.
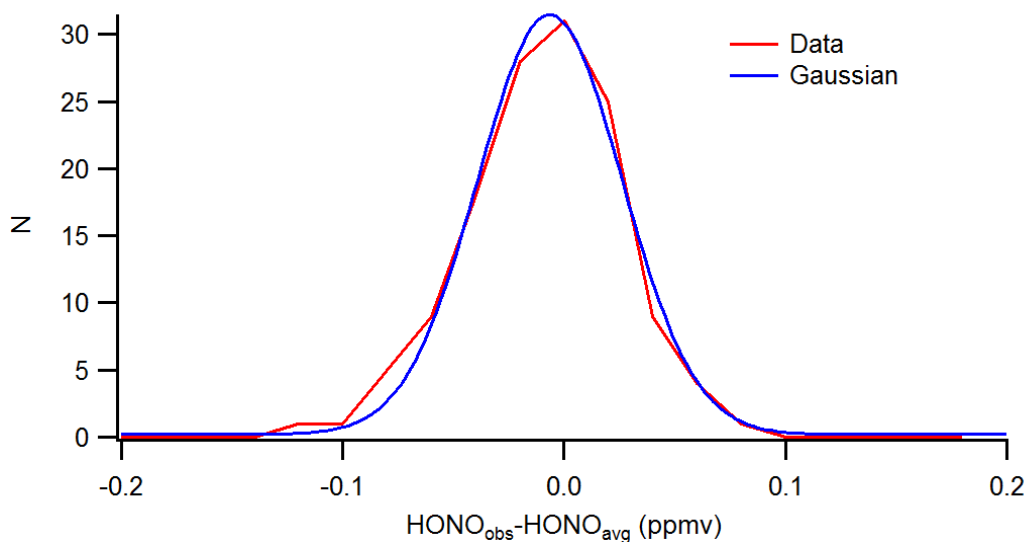
The above confirms that the output during the chosen period was stable (i.e., confirms that "the source output had stabilized" as we had stated in the caption of Figure 5), but it does not justify the choice of the left limit to what is called a stable period in Figure 5 (which we had estimated at 11:45:30).

Expanding on the above discussion, we applied a double exponential fit to the HONO data in Figure 5:
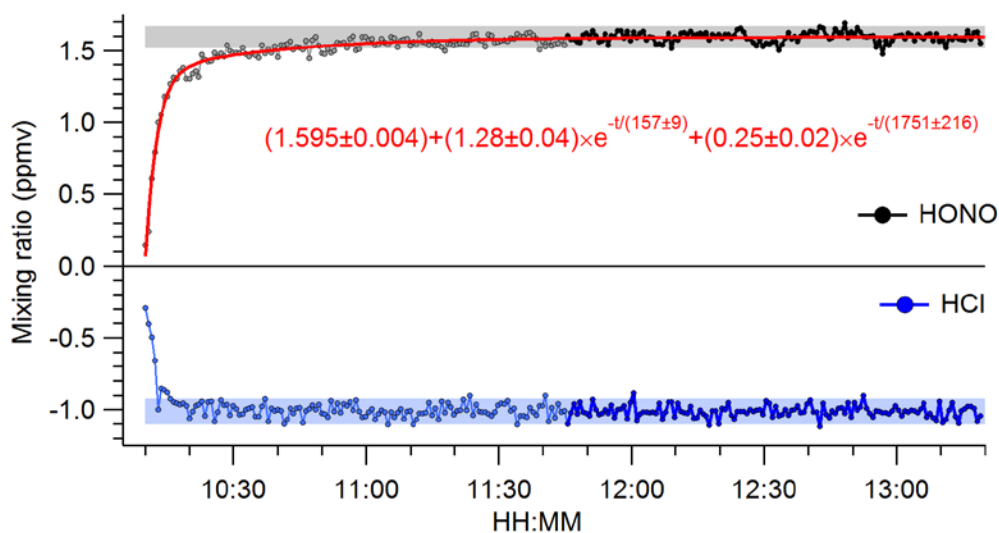
The first time constant of this fit was (157±9) s, corresponding to the mixing time of gas in the FTIR multipass cell (assuming plug flow 450 cm^3 at a flow rate of 170 cm^3 min^{-1} ~ 160 s). The second time constant was 29.3±3.6 min. The fit is within 1% of the limiting mean at 11:46:56 in Figure 5, which is very close to the "eye-ball" estimate.

We thank the reviewer for her/his time and comments, which are reproduced in *black italic font* below. Our responses are shown in regular font. Revised text (as it appears in the manuscript) is shown in blue font. Line numbers are those of the revised manuscript with changes accepted.

Anonymous Referee #2 Received and published: 12 June 2020

The authors present an optimized HONO calibration source that is based on the design of Febo et al., 1995, where HCl vapor is passed over solid NaNO2. They used a permeation tube to achieve lower (< 4 ppmv) HCl mixing ratios which is key to achieve higher purity as ClNO formation is slowed down. They quantified the impurities by using FTIR spectroscopy and TD-CRDS and found the optimized design of the source to be of > 97 % purity. With the optimized design (lower HCl supply) they were able to generate HONO concentrations in the low ppm range and by further dilution in the lower ppb range. The stabilization time of 1.5 h was short compared to other source designs.

Furthermore, the source is portable and after stabilization, HONO mixing ratios are readily tunable. Due to its instability, there are no permeation tubes or standard gases for HONO available and it must be produced in situ. Therefore, to calibrate gas phase mixing of HONO such a compact and easy deployable source is of interest for the atmospheric chemistry community. The study is well performed and the manuscript well written. Therefore, I support publication after considering the minor comments given below.

> Response: We appreciate the reviewer's supportive comments.

General comments:
As surfaces are unavoidable in laboratory setups, the role of surface reactions should be discussed. Although I guess that HONO formation from NO2 impurities is not of importance, there are also heterogeneous decomposition reactions for HONO that form NO (and NO2) and might therefore important to keep impurities low. See esp. (Finlayson-Pitts et al., 2003).

> Response: We agree with the reviewer that surface chemistry is an important consideration. Finlayson-Pitts et al. (2003) discussed the mechanism of heterogeneous conversion of NO_2 (to HONO and HNO_3) on Pyrex which involves formation and wall-adsorption of NO_2 dimer (i.e., N_2O_4) as the initial steps. Another paper by the same group (Syomin and Finlayson-Pitts, 2003) discusses HONO decomposition on glass surfaces, which was linked to wall-adsorbed HONO reacting with wall-adsorbed HNO_3.

> We believe this chemistry is limited in our setup as we have taken several steps to avoid it becoming factor. First of all, the chemistry described by Finlayson-Pitts et al. (2003) and Syomin and Finlayson-Pitts (2003) was observed in a static system on a time scale of hours or required cell conditioning with HNO_3; in our system, the 50 mL reaction vessel was continuously flushed (at a flow of ~150 mL min^{-1} from the zero air generator when in use and continuously with ~20 mL min^{-1} from the O_2 cylinder), such that there was little time for this chemistry to create much of an effect. In addition, formation of N_2O_4 scales with the square of the NO_2 concentration, which was low in our experiments. More importantly, the Pyrex reaction vessel was heated, which promotes partitioning of wall-adsorbed species to the gas-phase and reduces the extent of surface chemistry. Furthermore, the equilibrium

constant for the reaction $2NO_2 \rightleftharpoons N_2O_4$ is temperature-dependent favoring N_2O_4 dissociation at higher temperature. The NASA-JPL compilation recommends an equilibrium constant of 5.9×10^{-29} cm^3 molecule^{-1} e$^{(6643/T)}$ (Burkholder et al., 2015). When the temperature is increased from room temperature to 50 °C, the equilibrium constant decreases by a factor of ~6.

The following was added to the manuscript on line 97:

"In the second source ("source 2"), the NaNO$_2$ was placed in a two-neck, 50 mL Pyrex round bottom flask which was covered in aluminium foil to prevent photolysis of nitrite and nitrous acid and was externally heated to a temperature of 50 °C using a water bath and mechanically agitated using a magnetic stir bar as described by Febo et al. (1995). Heating this vessel promotes dissociation of molecular clusters such as N_2O_4 and partitioning of wall-adsorbed molecules to the gas-phase, which, if present, can drive HONO decomposition on borosilicate glass surfaces (Syomin and Finlayson-Pitts, 2003)."

Another consideration is surface chemistry in the connecting tubing. We constructed all our connecting tubing out of inert Teflon material and kept it under continuous flow (with an inert gas such as N_2 or O_2) when not in use (a detail we added to the manuscript - see our response to the question on L88 below).

Regarding the FTIR measurements: Can the authors provide more details about the reference spectrum used for HONO (spectrum of cis or trans isomer or total spectrum? taken at which temperature?). The spectral features will change with temperature as the amounts of cis and trans isomers of HONO change with temperature (e.g. Barney et al., 2000). Furthermore, please provide temperature and humidity values of the gas stream if possible.

Response: The reference spectrum was obtained from the Pacific Northwest National Laboratory digital library (Sharpe et al., 2004). According to their meta data file, they acquired this spectrum at 25 °C and atmospheric pressure and with dry nitrogen as diluent gas and generated HONO in situ from the reaction of NaNO$_2$ with HCl. We would hence expect the same distribution of HONO isomers as we would have generated in our experiments, which were conducted at room temperature.

We added more detail to section 2.2 ("Analysis of HONO source output by FTIR") on line 115 as requested by the reviewer:

"Room-temperature spectra were acquired continuously at a time resolution of 30 s. …. Mixing ratios of trace gases were determined from fits (by least squares error minimization over a selected wavelength range) of room-temperature reference spectra from the Pacific Northwest National Laboratory (Sharpe et al., 2004), …. the pressure inside the multi-pass cell (which was equal to that of the room) was monitored using a pressure transducer (Omegadyne PX419–015A5V)."

Because the bulk of the diluent gas was generated by passing room air through a scrubber, the relative humidity of the gas was approximately the same as the room (~30%; accounting for dilution with dry oxygen and neglecting H$_2$O co-emitted by the HCl perm tube, RH is estimated at ~25% for the data shown in Figure 2). Since the background spectrum was acquired with this H$_2$O background, the FTIR only shows drifts in H$_2$O. The following was added on line 187:

"A sample FTIR spectrum of this source's output is shown in Figure 2. With a freshly prepared HCl permeation tube and an estimated relative humidity in the round bottom flask of ~25%, > ~2.5 ppmv HCl were consumed and ~3.0 ppmv of HONO were produced. "

Specific comment:
L88: Why diluting with 20 mL min-1 flow of oxygen?

Response: The additional flow is probably not essential, but we found it practical to keep part of the setup under flow of a clean gas - our laboratory air contains surprisingly high levels of NO_x delivered from the building's air intake, plus the continued flow would remove any impurities that might build up. The use of a second mass flow controller was also advantageous as it allowed the residence time and HCl concentration to be changed on the fly without disturbing the permeation tube setup (which can take quite a long time to return to a stable output when flows are changed).

We modified the text as follows:

"The permeation tube was placed inside a glass chamber (VICI Dynacalibrator Model 120) whose temperature was controlled at 25.0 °C and which was continuously flushed at a flow rate of ~0.15 L min^{-1} with room air scrubbed using activated charcoal for a period of several days into a fume hood. The use of scrubbed air ensured that the gas stream contained water to maintain efficient HONO production (Schiller et al., 2001). The HCl output was diluted in a gas stream of O_2 (~20 mL min^{-1}); this gas stream also served to continuously flush the connecting tubing when not in use."

References:
Barney, W. S., Wingen, L. M., Lakin, M. J., Brauers, T., Stutz, J. and Finlayson-Pitts, B. J.: Infrared Absorption Cross-Section Measurements for Nitrous Acid (HONO) at Room Temperature, J. Phys. Chem. A, 104, 1692–1699, 2000.
Febo, A., Perrino, C. and Sparapani, M. Gherardi. R.: Evaluation of a High-Purity and High-Stability Continuous Generation System for Nitrous Acid, Environ. Sci. Technol, 29, 2390–2395, 1995.
Finlayson-Pitts, B. J., Wingen, L. M., Sumner, A. L., Syomin, D. and Ramazan, K. A.: The heterogeneous hydrolysis of NO2 in laboratory systems and in outdoor and indoor atmospheres: An integrated mechanism, Phys. Chem. Chem. Phys., 5, 223-242, 2003.
Burkholder, J. B., Sander, S. P., Abbatt, J. P. D., Barker, J. R., Huie, R. E., Kolb, C. E., Kurylo, M. J., Orkin, V. L., Wilmouth, D. M., and Wine, P. H.: Chemical Kinetics and Photochemical Data for Use in Atmospheric Studies, Evaluation Number 18, National Aeronautics and Space Administration, Jet Propulsion Laboratory, California Institute of Technology, Pasadena, California, 2015.
Schiller, C. L., Locquiao, S., Johnson, T. J., and Harris, G. W.: Atmospheric measurements of HONO by tunable diode laser absorption spectroscopy, J. Atmos. Chem., 40, 275-293, 10.1023/A:1012264601306, 2001.
Sharpe, S. W., Johnson, T. J., Sams, R. L., Chu, P. M., Rhoderick, G. C., and Johnson, P. A.: Gas-phase databases for quantitative infrared spectroscopy, Appl. Spectrosc., 58, 1452-1461, 2004.
Syomin, D. A., and Finlayson-Pitts, B. J.: HONO decomposition on borosilicate glass surfaces: implications for environmental chamber studies and field experiments, Phys. Chem. Chem. Phys., 5, 5236-5242, 10.1039/b309851f, 2003.

A compact, high-purity source of HONO validated by Fourier Transform Infrared and Thermal Dissociation Cavity Ring-down Spectroscopy

Nicholas J. Gingerysty[1] and Hans D. Osthoff[1]

[1] Department of Chemistry, University of Calgary, 2500 University Drive N.W., Calgary, Alberta, Canada T2N 1N4

5   *Correspondence to*: Hans D. Osthoff (hosthoff@ucalgary.ca)

Abstract

A well-characterized source of nitrous acid vapour (HONO) is essential for accurate ambient air measurements by instruments requiring external calibration. In this work, a compact HONO source is described in which gas streams containing dilute concentrations of HONO are generated by flowing
10   hydrochloric acid (HCl) vapour emanating from a permeation tube over continuously agitated dry sodium nitrite ($NaNO_2$) heated to 50 ℃. Mixing ratios of HONO and potential by-products including NO, NO_2 and nitrosyl chloride (ClNO) were quantified by Fourier Transform Infrared (FTIR) and thermal dissociation cavity ring-down spectroscopy (TD-CRDS). A key parameter is the concentration of HCl, which needs to be kept small (< 4 ppmv) to avoid ClNO formation. The source produces gas streams containing HONO in
15   air in > 957% purity relative to other nitrogen oxides. The source output is rapidly tuneable and stabilizes within 90 min. Combined with its small size and portability this source is highly suitable for calibration of HONO instruments in the field.

1 Introduction

The generation of nitrous acid vapour ($HONO_{(g)}$) free of other nitrogen oxides has been a long-standing challenge to atmospheric chemists (Table 1). Such sources are needed in kinetic studies, for absorption cross-section measurements, and for the calibration of field instruments. Nitrous acid is not suitable for permeation devices since HONO is difficult to prepare in low concentration and in high purity and disproportionates to nitric oxide and nitrogen dioxide via equilibrium (1).

$$NO_{(g)} + NO_{2(g)} + H_2O_{(g)} \rightleftharpoons 2HONO_{(g)} \qquad \text{(R1, R-1)}$$
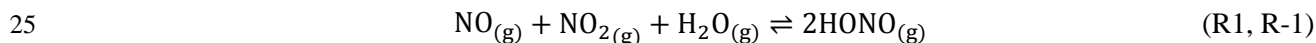
In fact, early experiments relied on the NO, NO_2 and H_2O vapour equilibrium to form HONO in situ (King and Moule, 1962; Cox, 1974; Stockwell and Calvert, 1978).

Cox and Derwent prepared HONO vapours in ~50% purity by flowing nitrogen over an aqueous solution containing 0.1 M sodium nitrite with and 1.4%-2.5% sulfuric acid (Cox and Derwent, 1976).

$$H_2SO_{4(aq)} + 2NaNO_{2(aq)} \rightarrow 2HONO_{(g)} + 2NaHSO_{4(aq)} \qquad \text{(R2)}$$
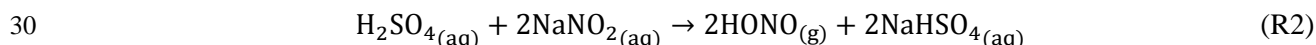
Braman and de la Cantera sublimed oxalic acid onto solid sodium nitrite and were able to produce gas streams in >50% and up to 90% purity as long as water was present (Braman and De la Cantera, 1986).

$$H_2C_2O_{4(g)} + NaNO_{2(s)} \xrightarrow{H_2O} HONO_{(g)} + NaHC_2O_{4(s)} \qquad \text{(R3)}$$
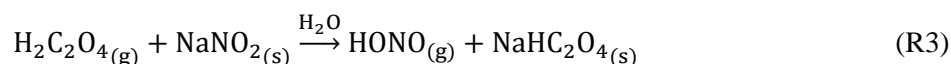
Subsequent refinements included a flow reactor design in solutions of sulfuric acid and sodium nitrite were dynamically mixed, producing a stable output in >90% purity (Taira and Kanda, 1990).

Febo et al. (1995) developed a method in which gas-phase hydrochloric acid emitted from a permeation device was quantitatively reacted in a humidified gas stream with solid sodium nitrite, producing a stable and highly pure (>99.5%) HONO output.

$$HCl_{(g)} + NaNO_{2(s)} \xrightarrow{H_2O} HONO_{(g)} + NaCl_{(s)} \qquad \text{(R4)}$$
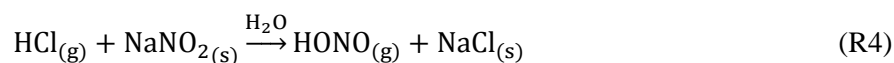
The output of sources based on R4 has been characterized by differential optical absorption spectroscopy (DOAS) (Febo et al., 1995; Stutz et al., 2000), Fourier transform infrared (FTIR) spectroscopy (Brust et al., 2000; Schiller et al., 2001), tuneable diode laser absorption spectroscopy (TLDAS) (Schiller et al., 2001), incoherent cavity-enhanced absorption spectroscopy (IBBCEAS) (Roberts et al., 2010), and long-path optical absorption photometry (LOPAP) (Ren et al., 2010). Stutz et al. (2000) noted that concentrations of

45 HONO should be kept low ($< 10^{14}$ molecules cm^{-3}; ~4 ppmv) to avoid disproportionation of HONO via R-1.

Perez et al. (2007) examined a source based on the design by Febo et al. (1995) using thermal-dissociation chemiluminescence (TD-CL) detection of NO and reported that their source co-emitted nitrosyl chloride (ClNO); they opted to generate HONO from reaction of H_2SO_4 aerosol with $NaNO_2$(s) instead. In contrast,
50 Roberts et al. (2010) observed little or no production of ClNO (<4.5%) and quantitative conversion of HCl to HONO, at odds with Perez et al. (2007) but in agreement with the original work by Febo et al. (1995). As far as we know, this inconsistency is unexplained to date.

As part of our development of an IBBCEAS for HONO measurement, our lab recently constructed a HONO source using an aqueous solution of $NaNO_2$ buffered with oxalate to pH 3.74 (Jordan and Osthoff, 2020).
55 This source generated HONO in trace amounts suitable to our needs but co-emitted NO and NO_2 in similar ratios as reported by Braman and De la Cantera (1986). Furthermore, this type of source could not be turned off (i.e., had to remain under continuous N_2 flow) and required long times to stabilize, motivating us to develop an alternative HONO generation method. Ambient air HONO measurement techniques that need to be externally calibrated often poorly agree with each other (Crilley et al., 2019), further motivating the
60 development of a well-characterized, compact and portable HONO source and to improve the understanding of conditions needed to suppress formation of undesired side products such as ClNO.

In this work, we describe the implementation of a compact, high-purity HONO generation device based on R4 for field deployment and laboratory experiments and characterized its output by FTIR and thermal dissociation cavity ring-down spectroscopy (TD-CRDS). Conditions to avoid generation of impurities such
65 as ClNO are identified. The performance of this source in comparison to existing methods is discussed.

2 Materials and methods

2.1. Generation of gas streams containing HONO

A practical challenge is the generation of stable and dilute gas streams containing HCl. Calibration gas
70 cylinders are the most straightforward method to use for this purpose but may require periods of up to 10 days to stabilize (Roberts et al., 2010). Furthermore, low-concentration HCl gas cylinders are expensive to source, such that we chose to generate HCl gas through the use of relatively inexpensive permeation devices.

In the setup by Febo et al. (1995), which was also implemented by Brust et al. (2000), Stutz et al. (2000) and Ren et al. (2010), a gas stream of N_2 is passed through Teflon tubing immersed in an HCl bath. This setup involved a rather large 1 L vessel containing liquid HCl which is somewhat impractical and potentially hazardous in a field setting. With portability in mind, we decided to construct a permeation tube containing HCl(l). Literature does not inform as to suitable tube dimensions, which were determined through trial-and-error.

Three HONO sources were constructed and evaluated. In the first ("source 1"), a 24 cm long, polytetrafluoroethylene (PTFE) permeation tube (Chromatographic Specialties C111LE; wall thickness 1.5 mm; outer diameter (o.d.) 7.8 mm) was filled with 2.5 mL of 37% HCl (Sigma-Aldrich) and sealed at both ends with PTFE plugs held in place by stainless steel compression rings. The permeation tube was placed inside a glass chamber (VICI Dynacalibrator Model 120) whose temperature was controlled at 25.0 °C and which was continuously flushed at a flow rate of ~0.15 L min^{-1} with room air scrubbed using activated charcoal for a period of several days into a fume hood. The use of scrubbed air ensured that the gas stream contained water to maintain efficient HONO production (Schiller et al., 2001). For the experiments shown in this manuscript, the relative humidity of the diluent gas stream was in the range of 15% to 35%.

The HCl output was diluted in a gas stream of O_2 (~20 mL min^{-1}); this gas stream also served to continuously flush the connecting tubing when not in use. Roughly 1.5 g of solid $NaNO_2$ was placed inside a 50 cm long loop of 3/16" (0.476 cm) inner diameter (i.d.) and ¼" (0.635 cm) o.d. fluorinated ethylene propylene (FEP) Teflon tubing downstream from the HCl addition point. This section could be manually bypassed with a pair of 3-way valves (Entegris) to turn HONO production on or off. A Teflon filter (Pall, 2 µm pore size and 47 mm diameter) inside a Teflon filter holder (Cole-Parmer) was placed downstream of the $NaNO_2$ powder.

In the second source ("source 2"), the $NaNO_2$ was placed in a two-neck, 50 mL Pyrex round bottom flask which was covered in aluminium foil to prevent photolysis of nitrite and nitrous acid and was externally heated to a temperature of 50 °C using a water bath and mechanically agitated using a magnetic stir bar as described by Febo et al. (1995). Heating this vessel promotes dissociation of molecular clusters such as N_2O_4 and partitioning of wall-adsorbed molecules to the gas-phase, which, if present, can drive HONO decomposition on borosilicate glass surfaces (Syomin and Finlayson-Pitts, 2003).

The third source ("optimized source") used the same setup as source 2, except that a shorter permeation tube (length 6 cm) containing 0.35 mL of HCl was used. This setup is depicted in Figure 1. The overall dimensions are 28 cm × 28 cm × 36 cm and its modular design ensures easy transport to and from the field.

To deliver HONO in atmospheric concentrations (i.e., < 10 ppbv), a portion of the source output was directed towards waste with the aid of a pump and a needle valve. The output concentration could be rapidly changed (typically by factors between 5 to 200) by adjusting the position of the needle valve. The remaining output was diluted using scrubbed air and directed towards the instruments at a final flow rate slightly larger than the sampling requirement of the instruments.

2.2 Analysis of HONO source output by FTIR

Gas streams exiting the HONO sources (prior to dilution) were analysed using an FTIR spectrometer (Bruker Tensor 27) equipped with a liquid nitrogen cooled mercury cadmium telluride (MCT) detector and a White multi-pass gas cell with a 6.4 m optical path length and an internal volume of 0.75 L (Gemini Scientific Instruments, Venus series) in a similar fashion as described earlier (Taha et al., 2013). Room-temperature spectra ~~Spectra~~ were acquired continuously at a time resolution of 30 s. Background spectra were recorded with HCl inline but with the $NaNO_2$ bypassed, which resulted in the observed spectra showing the change in trace gas concentrations.

Mixing ratios of trace gases were determined from fits (by least squares error minimization over a selected wavelength range) of room-temperature reference spectra from the Pacific Northwest National Laboratory (Sharpe et al., 2004), multiplied by the respective mixing ratios as variables, to the observed spectra. The reference spectra are provided in units of ppmv at atmospheric pressure per meter of optical length, necessitating a correction factor of 6.4 accounting for the actual path length and a pressure correction factor, for which the pressure inside the multi-pass cell (which was equal to that of the room) was monitored using a pressure transducer (Omegadyne PX419–015A5V).

The FTIR limits of detection (LODs) are specific to each molecule (due to differing absorption cross-sections) and are in the 100 to 300 parts-per-billion (by volume; ppbv; 10^{-9}) range. For example, the 1σ precision of NO_2 data was ±100 ppbv, yielding a 3σ LOD of 300 ppbv.

The spectral resolution of the FTIR was ~0.5 cm^{-1}, which does not suffice to fully resolve the absorption lines of HCl, H_2O and NO; their FTIR derived mixing ratios are hence lower limits.

2.3 Analysis of HONO source output by TD-CRDS

The (diluted) HONO source output was also analysed using a four-channel TD-CRDS instrument (Odame-Ankrah, 2015). Briefly, mixing ratios of NO_2 are quantified by absorption at 405 nm. Ring-down time constants in the absence (τ_0) and presence (τ) of NO_2 are converted to concentrations (N) using equation (2) where c is the speed of light, σ is the NO_2 absorption cross-section, and R_L is a correction factor (~1.2) accounting for mirror purge flows (Paul and Osthoff, 2010).

$$N = \frac{R_L}{c\sigma}\left(\frac{1}{\tau} - \frac{1}{\tau_0}\right) \tag{1}$$

Concentrations are converted to mixing ratios using the ideal gas law. Other NO_y components are converted to NO_2 in separate channels and are quantified by difference.

For this study, the instrument was operated as follows: Mixing ratios of NO_2 were monitored using a room temperature, 1/4" (0.64 cm) o.d. and 1/8" (0.32 cm) i.d. FEP Teflon inlet. Mixing ratios of NO_x were quantified on a second channel with a room temperature Teflon inlet and by adding O_3 (mixing ratio after addition ~3 ppmv) to titrate NO to NO_2 (Odame-Ankrah, 2015; Fuchs et al., 2009). A third channel was operated with a 1/4" (0.64 cm) o.d. quartz inlet heated to 600 °C. Ozone was added between the quartz inlet and the CRDS cell to quantify NO_y, including HONO (Jordan and Osthoff, 2020; Wild et al., 2014; Perez et al., 2007). The fourth inlet was operated at 350 °C and with added O_3. This channel quantified $NO_x + \Sigma PAN + \Sigma AN + ClNO + ClNO_2$ and was used as a HONO reference channel. Each channel sampled at a flow rate of ~0.8 slpm through ~5 cm short, 1/16" i.d. Teflon flow restrictors placed inline after the heated quartz sections (if existing) and before a 50 mm Teflon (Pall Teflo, 2 µm pore size) housed in a Teflon filter holder (Cole Parmer). The laser pulse repetition rate was 1500 Hz, and 1500 ring-down events were averaged to produce 1 s data.

2.4 Field deployment

The HONO source was utilized during the "Study of nitrogen oxides in winter downwind from oil and gas sands" (SNOWDOGS) field campaign in Fort McKay, Alberta, Canada, in January 2020. Its output was quantified in parallel by TD-CRDS and a Thermo 42i-Y NO-NOy CL instrument equipped with a Mo converter heated to 325 °C. This converter and the TD-CRDS quartz inlets were mounted on the roof of a trailer which housed the instruments and the HONO source. The TD-CRDS sampled at a flow rate of ~1.2 slpm per channel through ~5 cm short, 300 µm i.d. stainless steel flow restrictors placed inline after the heated quartz sections and before the Teflon filter assembly. The HONO source output was delivered via a 5 m long, 1/4" (0.64 cm) o.d. and 3/16" (0.48 cm) i.d. FEP Teflon tube to both instruments.
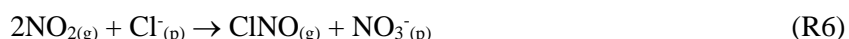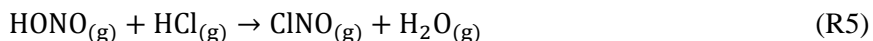
3 Results

3.1 Development of a compact, high-purity HONO source

165 The first design tested (source 1) produced an output of ~38 ppmv of HONO from a similar amount (>38 ppmv) of HCl (Figure S1A). This HONO mixing ratio is a factor of ~10 larger than the maximum recommended by Stutz et al. (2000) to avoid partial conversion of HONO to NO_2 and NO via ~~R5~~R-1. Consistently, the source output contained ~4.0 ppmv of NO_2 (Figure S1A) and an analogous amount of NO (Figure S1B). Furthermore, the spectrum contained an absorption feature around 1808 cm^{-1}, reproduced by

170 ~15.5 ppmv of ClNO.

Nitrosyl chloride can be produced by reaction of HONO with gas-phase or wall-adsorbed HCl (Zhang et al., 1996; Wingen et al., 2000) or by reaction of two equivalents of NO_2 with particulate phase Cl^- (Weis and Ewing, 1999), though the relatively low mixing ratios of NO_2 in this system makes this reaction less likely.

175
$$HONO_{(g)} + HCl_{(g)} \rightarrow ClNO_{(g)} + H_2O_{(g)} \tag{R5}$$

$$2NO_{2(g)} + Cl^-_{(p)} \rightarrow ClNO_{(g)} + NO_3^-_{(p)} \tag{R6}$$

The FTIR spectrum contained ~50 ppmv more H_2O than the reference spectrum, i.e., more moisture than emitted by the permeation tube with $NaNO_2$ bypassed. While this is consistent with ClNO production via ~~R6~~R5, the H_2O data are likely not meaningful since the H_2O mixing ratios changed slowly over time (data

180 not shown), possibly because of slow equilibration with the inner walls of the tubing and multi-pass cell and perhaps also because of water's presence in the FTIR optical path outside the multi-pass cell at a concentration that may have drifted.

Febo et al. (1995) reported lower production of NO_x by mechanically agitating the $NaNO_2$ using a stir bar (to break up pockets of high [HONO]) and by heating the reaction vessel to 50 °C; these steps were

185 incorporated in the second design (source 2). The FTIR spectrum of its output showed a consumption of > ~42 ppmv HCl and production of ~48 ppmv HONO, ~8.0 ppmv of NO_2, ~6.5 ppmv of ClNO, ~8 ppmv of NO, and ~50 ppmv of H_2O (Figure S2), an improvement over source 1 in terms of unwanted ClNO production but still inadequate.

A shorter HCl permeation tube was used in the third design, with the expectation that the lower HCl

190 concentrations results in reduced generation of side products via R5 and R6. A sample FTIR spectrum of this source's output is shown in Figure 2. With a freshly prepared HCl permeation tube and an estimated

relative humidity in the round bottom flask of ~25%, > ~2.5 ppmv HCl were consumed and ~3.0 ppmv of HONO were produced. The mixing ratios of undesired side products (i.e., NO, NO_2, ClNO, and HNO_3) were below their respective FTIR detection limits (Figures 2, S3 and S4).

195 **3.2 Analysis of source output by TD-CRDS**

To better constrain the mole fractions of impurities, the source output was analysed by TD-CRDS. Figure 3 shows an example experiment. The TD-CRDS sampled scrubbed air before 21:38 and after 21:58 to determine the ring-down time constants in the absence of absorbers, τ_0. In the time periods in between, varying amounts of the HONO output were sampled. There was little response other than in the NO_y
200 channel, the only channel sensitive to HONO. Scatter plots of NO_2, NO_x and $NO_x + \Sigma PAN + \Sigma AN + ClNO + ClNO_2$ ("HONO ref") against NO_y (Figure 3, inserts) have slopes of $(1.29\pm0.06)\%$, $(1.54\pm0.06)\%$ and $(2.28\pm0.04)\%$, respectively, from which a source purity of >97.3% was deduced.

When concentrations changed, the 90%-10% rise (and fall) times of the TD-CRDS was < 3 s, a time
205 constant identical to changes in NO_x concentration and indicating a "well-behaved" inlet, i.e., the absence of inlet memory effects and fast equilibration with the inner walls of the inlet. The fast response contrasts with the rise (and fall) times of HNO_3 of > 180 s (data not shown). Furthermore, the response in a channel sampling from an inlet heated to 600 °C without added O_3 was the same as the that of the NO_2 channel (data not shown), consistent with the absence of HNO_3 observed by FTIR spectroscopy (Figure S4).

210 A quartz inlet temperature scan when the TD-CRDS was sampling a constant concentration of HONO is shown in Figure 4. The experimental TD curve was reproduced by a fit to equation (2), which is based on equation (4) by Paul et al. (2009).

$$[Observed]_{total} = [NO_x] + [ClNO]\left(1 - e^{-A_{ClNO} \times e^{\frac{-E_{A,ClNO}}{RT}} \times t_{res}}\right) + [HONO]\left(1 - e^{-A_{HONO} \times e^{\frac{-E_{A,HONO}}{RT}} \times t_{res}}\right) \qquad (2)$$

Here, A_{HONO} and $E_{A,HONO}$ are Arrhenius parameters for the TD of HONO taken from Tsang (1991), A_{ClNO}
215 and $E_{A,ClNO}$ are from Baulch et al. (1981), and t_{res} is the residence time of the gas in the converter at the converter set temperature T. A fit of equation (2) to the observation (superimposed as a black line in Figure 4) using the software package Igor Pro (Wavemetrics) gave $t_{res} = (77.6\pm0.1)$ ms, $[NO_x] = (0.03\pm0.30)$ ppbv, $[ClNO] = (0.27\pm0.34)$ ppbv, and $[HONO] = (49.97\pm0.18)$ ppbv, suggesting a source purity of $(99.4\pm0.9)\%$.

In our experience, the TD inflection points vary between TD-CRDS channels (and depend on sample flow
220 rates), captured by the t_{res} parameter that is specific to each channel. For the data shown in Figure 4, HONO

fully dissociates at a temperature of ~570 °C, and the inflection point is at ~500 °C. Nitrosyl chloride is predicted to fully dissociate at ~330 °C (inflection point at ~288 °C), such that the temperature of 350 °C chosen for the HONO ref channel (Figure 3) is justified. The blue, dashed line superimposed in Figure 4 shows a simulation of 5 ppbv ClNO and 45 ppbv HONO to demonstrate the relative positions of the TD of

225 ClNO and HONO. We attempted to verify the ClNO TD profile experimentally, but the unoptimized source's ClNO outputs were not sufficiently stable, and those attempts were abandoned. Regardless, it is clear from Figure 4 that the contribution of ClNO to the total source output is negligible.

As can be seen from the insert in Figure 4, HONO contributes a tiny amount to the TD-CRDS signal at 350 °C (~4 pptv in the simulation of 50 ppbv HONO). This contribution may differ between quartz heaters

230 and channels and could have impacted by TD-CRDS using multiple parallel channels presented at the beginning of this section and in Figure 3, leading to an overestimation of the total amount of impurities present in that experiment. The temperature scan data shown in Figure 4, on the other hand, were collected using a single quartz heater and are thus more accurate.

3.3 Source stability

235 The source output gradually decreased over a time scale of weeks of continuous use, which was rationalized by the visible depletion of the HCl permeation tube. However, the source output remained stable and reproducible on shorter time scales. An example FTIR time series is shown in Figure 5, which was acquired after 1 month of intermittent use. After a 1.5 hours stabilization period, the source produced a stable output of 1.57 ppmv of HONO (from >1.0 ppmv of HCl) with a precision of ±35 ppbv.

240 **3.4 Source purity and day-to-day reproducibility**

The optimized source routinely delivered HONO in high purity (range 96.0% - 98.7%), as long as scrubbed, moisture-containing room air was used as diluent gas (Table 2). When dry cylinder gas was used instead, the source output was stable but contained a larger amount of undesired side products; for example, on July 25, 2019, the output contained 4.6% NO_2 and 8.8% NO + ClNO (Table 2). When used in the field, the

245 performance was similar: with scrubbed air, the HONO purity was 98.5%, whereas with dry cylinder gas, the purity was merely 81.3% (Table 2 and Figure S5).

4. Discussion

In this work, a small footprint, portable, stable, rapidly tuneable, and high-purity (>97% on average) HONO source has been described. The source achieves compactness by using a diffusion tube containing 0.35 mL concentrated HCl rather than a 1 L HCl bath. The latter is a considerable hazard since an HCl spill can cause severe burns of skin or permanent eye damage, and hydrochloric acid vapours are toxic to inhale. Hence, smaller volumes are preferred when deploying to the field. The source stabilizes within a time frame of 1.5 h (Figure 5) which is fast compared to, for example, the 10 day stabilization period reported by Roberts et al. (2010). The source output is also rapidly tuneable (Figure 3) which allows expedient generation of calibration plots. These properties make it a useful setup for in-field instrument calibrations.

The combination of FTIR and TD-CRDS provided a unique and powerful tool set to analyse the purity of the source's output. This work has shown that HONO sources based on R4 can generate NO, NO_2 and ClNO as by-products via R-1 and R5. Febo et al. (1995) and Roberts et al. (2010) have presented HONO sources based on R4 and demonstrated stoichiometric conversion of HCl to HONO. The results in this work suggest that devices relying solely on loss of HCl for calibration of HONO output should be used with caution as co-production of NO, NO_2, and ClNO is a real possibility. In our setup, formation of ClNO could be avoided by keeping the HCl concentration low (i.e., < 4 ppmv), which puts an important constraint on sources generating HONO by R4. With this in mind, it is instructive to scrutinize the earlier work in regard to side product formation. It has generally been noted that the presence of moisture is needed to ensure a high HONO output. We suggest that water is needed in part because ClNO is prone to hydrolysis (Karlsson and Ljungstrom, 1996) such that the product distribution is shifted towards HONO.

$$ClNO_{(g)} + H_2O_{(g)} \rightarrow HONO_{(g)} + HCl_{(g)} \tag{R-5}$$
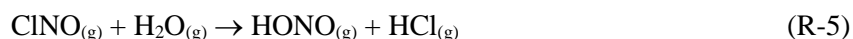
Roberts et al. (2010) observed no ClNO production, likely because they kept their concentrations relatively low (<900 ppbv) and humidified their gas streams, though they appear to be just below the threshold of possible ClNO production. Perez et al. (2007), on the other hand, observed ClNO but did not disclose details as to how they operated their source, i.e., if they worked under trace conditions and with humidified gases, though it is likely that either or both conditions were not met. Schiller et al. (2001) bubbled N_2 through liquid HCl and would have certainly achieved high enough HCl concentration to generate ClNO with their setup. However, they reported achieving higher HONO output in the presence of moisture. Hydrolysis of ClNO (R-5) may be a (partial) explanation why the presence of H_2O improved the output of their HONO.

The present HONO source has a large dynamic range (0 - 1 ppmv), well above the HONO concentrations found in ambient air. For field calibrations in future, it may be desirable to construct a permeation tube with lower HCl output, for example by lowering the HCl concentration in the permeation tube.

Data availability

The data used in this study are available from the corresponding author upon request (hosthoff@ucalgary.ca).

Author contributions

NJG and HDO designed the experiments and carried them out.

Competing interests

The authors declare that they have no conflict of interest.

Acknowledgments

References

Baulch, D. L., Duxbury, J., Grant, S. J., and Montague, D. C.: Evaluated kinetic data for high-temperature

295   reactions, vol. 4: Homogeneous gas-phase reactions of halogen-containing and cyanide-containing

species, J. Phys. Chem. Ref. Data, 10, Supplement 1, 1-721, 1981.

Braman, R. S., and De la Cantera, M. A.: Sublimation sources for nitrous acid and other nitrogen

compounds in air, Anal. Chem., 58, 1533-1537, 10.1021/ac00298a059, 1986.

Brust, A. S., Becker, K. H., Kleffmann, J., and Wiesen, P.: UV absorption cross sections of nitrous acid,

300   Atmos. Environm., 34, 13-19, 10.1016/S1352-2310(99)00322-2, 2000.

Cox, R. A.: The photolysis of gaseous nitrous acid, Journal of Photochemistry, 3, 175-188, 10.1016/0047-2670(74)80018-3, 1974.

Cox, R. A., and Derwent, R. G.: The ultra-violet absorption spectrum of gaseous nitrous acid, Journal of

Photochemistry, 6, 23-34, 10.1016/0047-2670(76)87004-9, 1976.

305   Crilley, L. R., Kramer, L. J., Ouyang, B., Duan, J., Zhang, W., Tong, S., Ge, M., Tang, K., Qin, M., Xie,

P., Shaw, M. D., Lewis, A. C., Mehra, A., Bannan, T. J., Worrall, S. D., Priestley, M., Bacak, A., Coe, H.,

Allan, J., Percival, C. J., Popoola, O. A. M., Jones, R. L., and Bloss, W. J.: Intercomparison of nitrous

acid (HONO) measurement techniques in a megacity (Beijing), Atmos. Meas. Tech., 12, 6449-6463,

10.5194/amt-12-6449-2019, 2019.

310   Febo, A., Perrino, C., Gherardi, M., and Sparapani, R.: Evaluation of a High-Purity and High-Stability

Continuous Generation System for Nitrous Acid, Environm. Sci. Technol., 29, 2390-2395,

10.1021/es00009a035, 1995.

Fuchs, H., Dubé, W. P., Lerner, B. M., Wagner, N. L., Williams, E. J., and Brown, S. S.: A Sensitive and

Versatile Detector for Atmospheric NO_2 and NO_x Based on Blue Diode Laser Cavity Ring-Down

315   Spectroscopy, Environm. Sci. Technol., 43, 7831-7836, 10.1021/es902067h, 2009.

Jordan, N., and Osthoff, H. D.: Quantification of nitrous acid (HONO) and nitrogen dioxide (NO_2) in

ambient air by broadband cavity-enhanced absorption spectroscopy (IBBCEAS) between 361 and 388

nm, Atmos. Meas. Tech., 13, 273-285, 10.5194/amt-13-273-2020, 2020.

Karlsson, R. S., and Ljungstrom, E. B.: Laboratory study of ClNO: Hydrolysis, Environm. Sci. Technol.,

320   30, 2008-2013, 10.1021/es950801f, 1996.

King, G. W., and Moule, D.: The ultraviolet absorption spectrum of nitrous acid in the vapor state,

Canadian Journal of Chemistry, 40, 2057-2065, 10.1139/v62-316, 1962.

Odame-Ankrah, C. A.: Improved detection instrument for nitrogen oxide species, Ph.D., Chemistry,

University of Calgary, http://hdl.handle.net/11023/2006, 10.5072/PRISM/26475, Calgary, 2015.

325   Paul, D., Furgeson, A., and Osthoff, H. D.: Measurements of total peroxy and alkyl nitrate abundances in laboratory-generated gas samples by thermal dissociation cavity ring-down spectroscopy, Rev. Sci. Instrum., 80, 114101, 10.1063/1.3258204 2009.

Paul, D., and Osthoff, H. D.: Absolute Measurements of Total Peroxy Nitrate Mixing Ratios by Thermal Dissociation Blue Diode Laser Cavity Ring-Down Spectroscopy, Anal. Chem., 82, 6695-6703,

330   10.1021/ac101441z, 2010.

Perez, I. M., Wooldridge, P. J., and Cohen, R. C.: Laboratory evaluation of a novel thermal dissociation chemiluminescence method for in situ detection of nitrous acid, Atmos. Environm., 41, 3993-4001, 10.1016/j.atmosenv.2007.01.060, 2007.

Reed, C., Brumby, C. A., Crilley, L. R., Kramer, L. J., Bloss, W. J., Seakins, P. W., Lee, J. D., and

335   Carpenter, L. J.: HONO measurement by differential photolysis, Atmos. Meas. Tech., 9, 2483-2495, 10.5194/amt-9-2483-2016, 2016.

Ren, X., Gao, H., Zhou, X., Crounse, J. D., Wennberg, P. O., Browne, E. C., LaFranchi, B. W., Cohen, R. C., McKay, M., Goldstein, A. H., and Mao, J.: Measurement of atmospheric nitrous acid at Bodgett Forest during BEARPEX2007, Atmos. Chem. Phys., 10, 6283-6294, 10.5194/acp-10-6283-2010, 2010.

340   Roberts, J. M., Veres, P. R., Warneke, C., Neuman, J. A., Washenfelder, R. A., Brown, S. S., Baasandorj, M., Burkholder, J. B., Burling, I. R., Johnson, T. J., Yokelson, R. J., and de Gouw, J.: Measurement of HONO, HNCO, and other inorganic acids by negative-ion proton-transfer chemical-ionization mass spectrometry (NI-PT-CIMS): application to biomass burning emissions, Atmospheric Measurement Techniques, 3, 981-990, 10.5194/amt-3-981-2010, 2010.

345   Schiller, C. L., Locquiao, S., Johnson, T. J., and Harris, G. W.: Atmospheric measurements of HONO by tunable diode laser absorption spectroscopy, J. Atmos. Chem., 40, 275-293, 10.1023/A:1012264601306, 2001.

Sharpe, S. W., Johnson, T. J., Sams, R. L., Chu, P. M., Rhoderick, G. C., and Johnson, P. A.: Gas-phase databases for quantitative infrared spectroscopy, Appl. Spectrosc., 58, 1452-1461, 2004.

350   Stockwell, W. R., and Calvert, J. G.: The near ultraviolet absorption spectrum of gaseous HONO and N_2O_3, Journal of Photochemistry, 8, 193-203, 10.1016/0047-2670(78)80019-7, 1978.

Stutz, J., Kim, E. S., Platt, U., Bruno, P., Perrino, C., and Febo, A.: UV-visible absorption cross sections of nitrous acid, J. Geophys. Res., 105, 14585-14592, 10.1029/2000JD900003, 2000.

Taha, Y. M., Odame-Ankrah, C. A., and Osthoff, H. D.: Real-time vapor detection of nitroaromatic

355   explosives by catalytic thermal dissociation blue diode laser cavity ring-down spectroscopy, Chem. Phys. Lett., 582, 15-20, 10.1016/j.cplett.2013.07.040, 2013.

Taira, M., and Kanda, Y.: Continuous generation system for low-concentration gaseous nitrous acid, Anal. Chem., 62, 630-633, 10.1021/ac00205a018, 1990.

Tsang, W., and Herron, J. T.: Chemical Kinetic Data Base for Propellant Combustion I. Reactions

360   Involving NO, NO$_2$, HNO, HNO$_2$, HCN and N$_2$O, J. Phys. Chem. Ref. Data, 20, 609-663, 10.1063/1.555890, 1991.

Weis, D. D., and Ewing, G. E.: The Reaction of Nitrogen Dioxide with Sea Salt Aerosol, J. Phys. Chem. A, 103, 4865-4873, 10.1021/jp984488q, 1999.

Wild, R. J., Edwards, P. M., Dube, W. P., Baumann, K., Edgerton, E. S., Quinn, P. K., Roberts, J. M.,

365   Rollins, A. W., Veres, P. R., Warneke, C., Williams, E. J., Yuan, B., and Brown, S. S.: A Measurement of Total Reactive Nitrogen, NO$_y$, together with NO$_2$, NO, and O$_3$ via Cavity Ring-down Spectroscopy, Environm. Sci. Technol., 48, 9609-9615, 10.1021/es501896w, 2014.

Wingen, L. M., Barney, W. S., Lakin, M. J., Brauers, T., and Finlayson-Pitts, B. J.: A unique method for laboratory quantification of gaseous nitrous acid (HONO) using the reaction HONO+HCl -> ClNO+H2O,

370   J. Phys. Chem. A, 104, 329-335, 10.1021/jp992890e, 2000.

Zhang, R., Leu, M.-T., and Keyser, L. F.: Heterogeneous Chemistry of HONO on Liquid Sulfuric Acid: A New Mechanism of Chlorine Activation on Stratospheric Sulfate Aerosols, The Journal of Physical Chemistry, 100, 339-345, 10.1021/jp952060a, 1996.
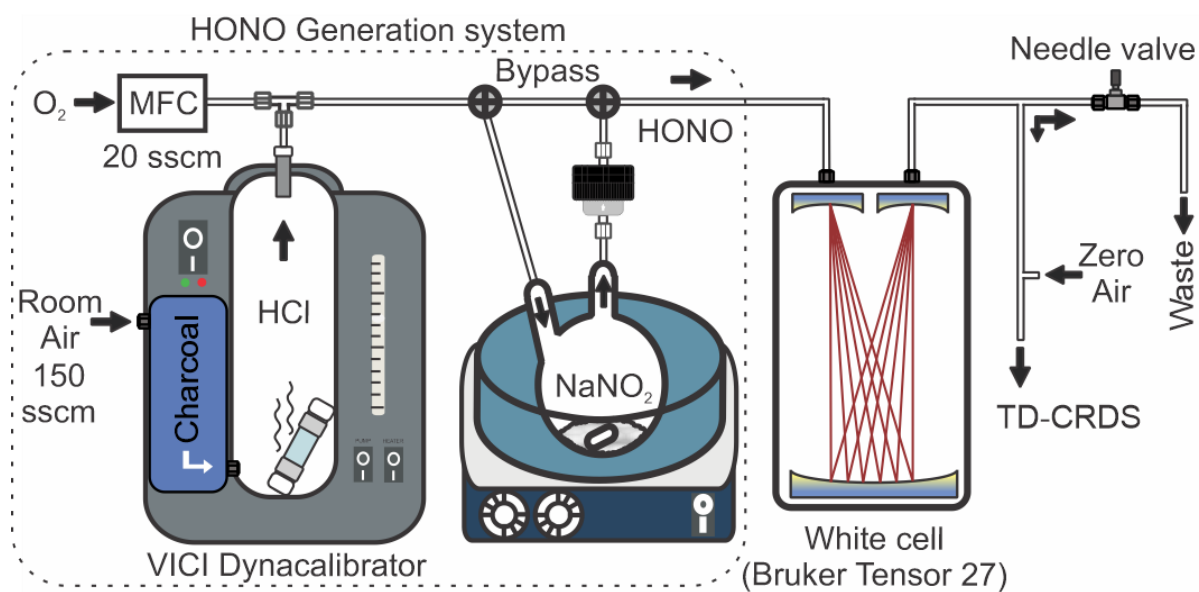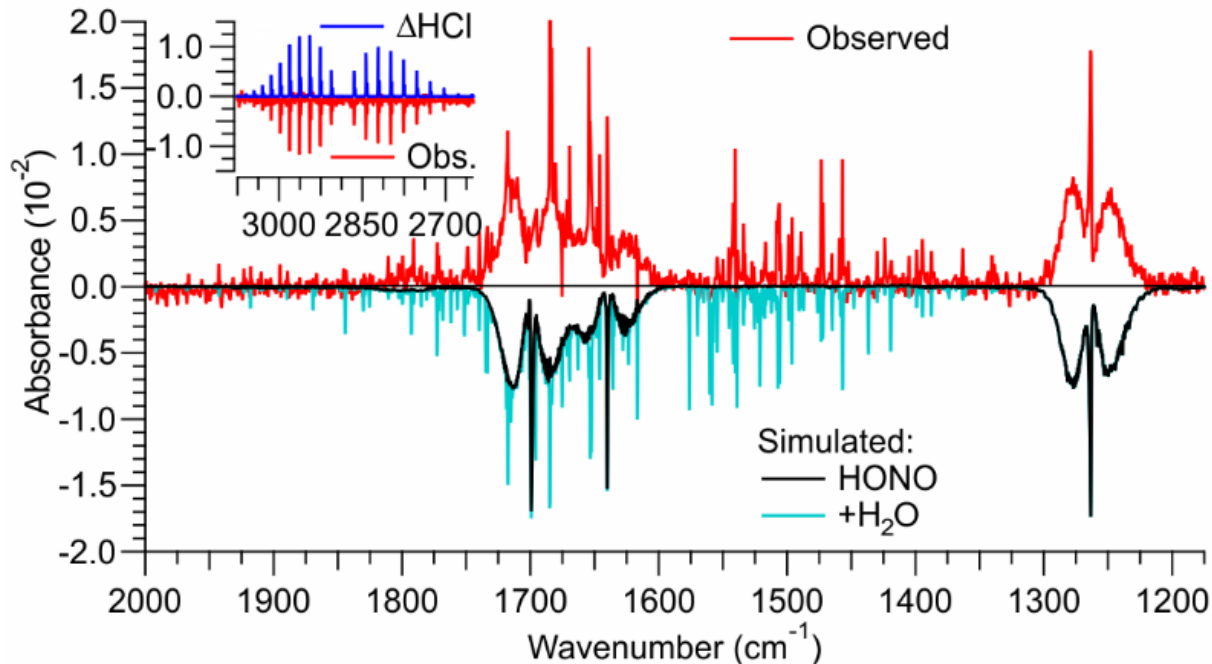

375

Figure 1. Schematics of the experimental setup. The high-purity HONO generation system is shown on the left (dotted border). MFC = mass flow controller. sccm = standard cubic centimetre per minute.

Figure 2. Infrared spectrum (shown in red colour) of a gas stream containing HONO generated by reaction of $HCl_{(g)}$ with $NaNO_{2(s)}$ after the source was optimized. The reference spectrum was collected when $NaNO_2$ was bypassed, i.e., contained HCl. Literature spectra (Sharpe et al., 2004) were multiplied by the optical path length of 6.4 m and mixing ratios of the identified trace gases until they reproduced the observed spectrum. The optimized source delivered 3.0 ppmv of HONO from >2.5 ppmv of HCl. The spectrum also contained ~4.0 ppmv of H_2O. The HCl and H_2O concentrations are underestimates of their true concentrations since their absorption lines are narrower than the resolution of the FTIR of 0.5 cm^{-1}.
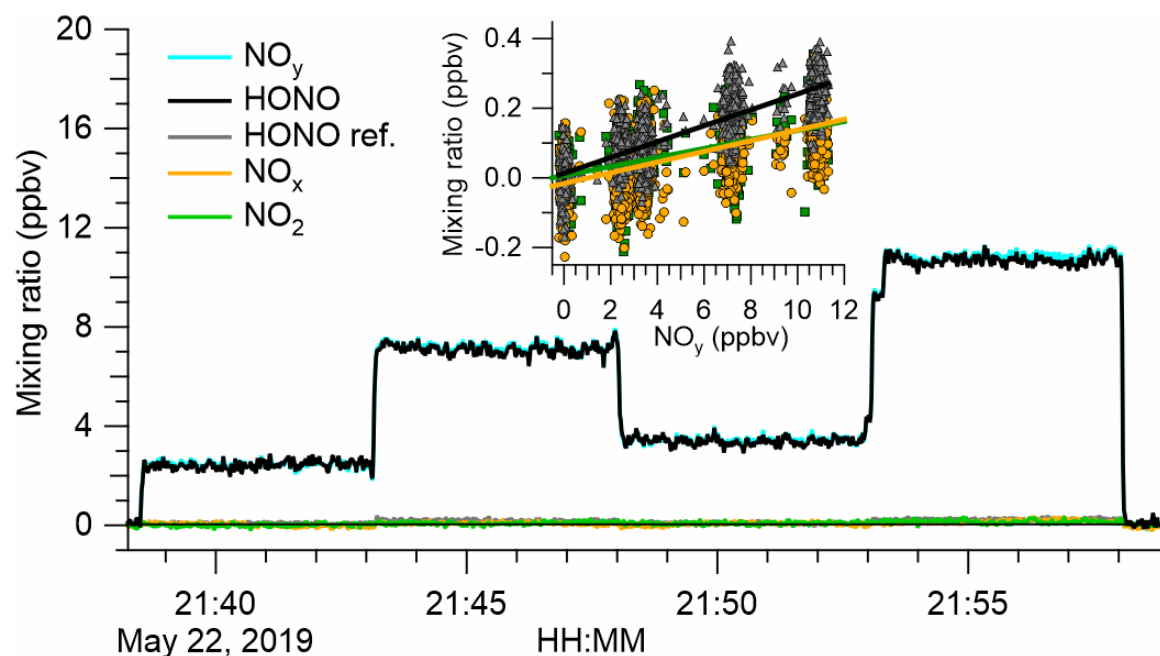
Figure 3. Analysis of the HONO source output by TD-CRDS. The TD-CRDS sampled scrubbed "zero" air before 21:38 and after 21:58. The HONO source output was varied by incrementally opening (or closing) the bypass valve. The HONO mixing ratio was calculated by subtracting the response of the "HONO reference" from the NO_y channel. The insert shows scatter plots of NO_2, NO_x and "HONO ref" against NO_y. Slopes of $(1.29\pm0.06)\%$ for NO_2 (points shown in green), $(1.54\pm0.06)\%$ for NO_x (data points shown in orange) and $(2.28\pm0.04)\%$ for "HONO ref") (points shown in grey) were determined, respectively.
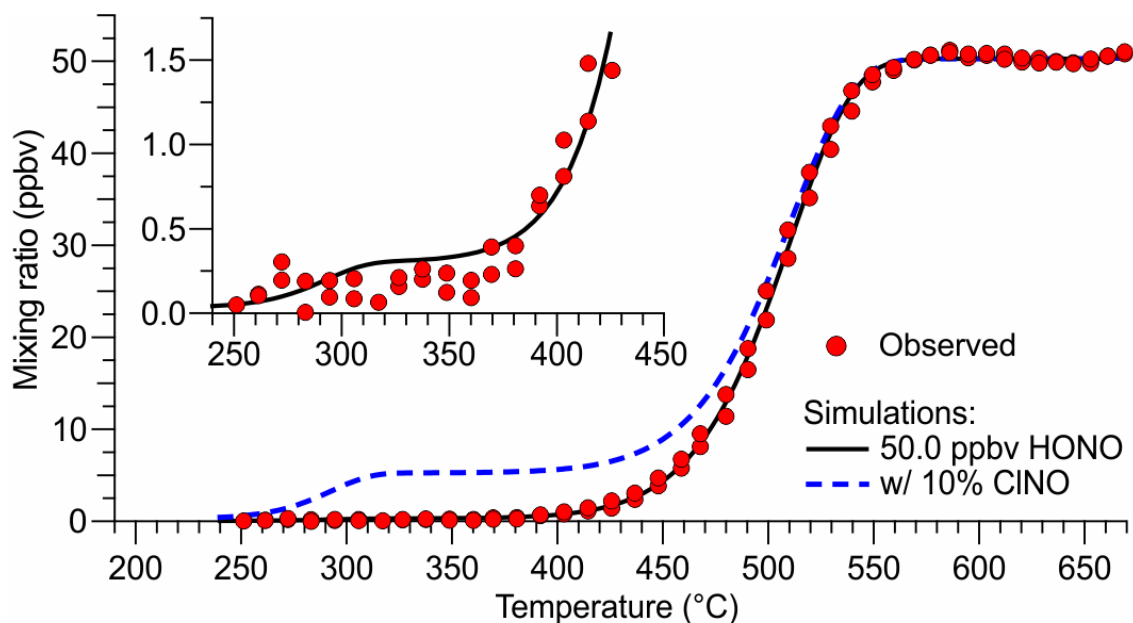
Figure 4. Inlet temperature scan when the TD-CRDS was sampling a constant concentration of HONO (data points shown in red). The TD profile was reproduced by a fit to equation (2) with mixing ratios of (49.97±0.18) ppbv, (0.27±0.34) ppbv and (0.03±0.30) ppbv for HONO, ClNO and NO_x, respectively (black line). The blue dashed line shows the predicted TD curve of a hypothetical mixture containing 5.0 ppbv ClNO and 45.0 ppbv HONO. The insert shows a close-up of the temperature region in which TD of ClNO occurs.
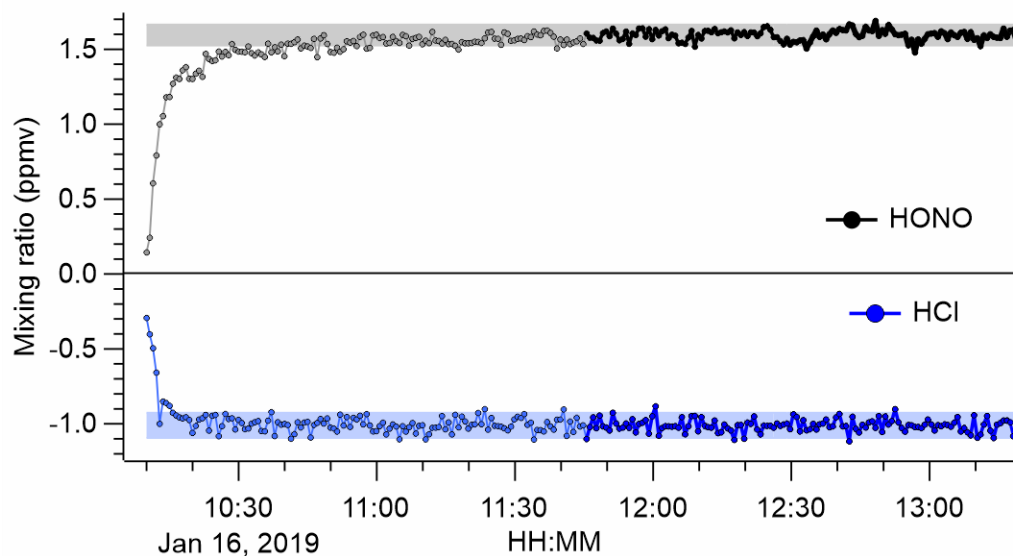
Figure 5. Time series of HONO and HCl mixing ratios derived from FTIR analysis of the undiluted HONO source output. The NaNO$_2$ was placed in line at 10:10. ~~Data acquired during the initial period are shown in light grey colour.~~ The shaded areas represent the average $\pm$ 2σ after the source output ~~had~~ was judged to have stabilized (after 11:45; data points shown in black colour). The 1σ precision of the HONO data was $\pm$~~35~~ 35 ppbv and that of the HCl data was $\pm$42 ppbv. The HCl mixing ratios are an underestimate because the widths of their absorption lines are less than the FTIR's resolution of 0.5 cm^{-1}.

Table 1. Selected HONO generation systems described in the literature. n/d = not disclosed

Reference	Method	Analytical method	Result	Notes
(King and Moule, 1962; Stockwell and Calvert, 1978)	(R1)	UV absorption	mixture of NO, NO_2 and HONO	Equilibration of (R1)
(Cox, 1974)	(R1)	NO and "total NO_x" CL; HONO scrubbed w/ NaOH(0.1N)	mixture of NO, NO_2 and HONO	Equilibration of (R1)
(Cox and Derwent, 1976)	(R2)	NO and "total NO_x" CL; HONO scrubbed w/ NaOH(0.1N)	mixture of NO, NO_2 and ~50% HONO	Volatilization of "nitrous fumes" from solution of sulfuric acid and sodium nitrite
(Braman and De la Cantera, 1986)	(R3)	NO/NO_y CL analyser (heated Au tube)	mixture of NO, NO_2 and 50% - 90% HONO	Sublimation of oxalic acid on sodium nitrite
(Taira and Kanda, 1990)	(R2)	NO/NO_y CL analyser (carbon converter); HONO collected on Na_2CO_3 filters and analysed by IC	mixture containing 2% - 3% NO and 4% - 6% NO_2	Volatilization of HONO from dynamically mixed sodium nitrite and sulfuric acid solution
(Febo et al., 1995; Stutz et al., 2000)	(R4)	DOAS (NO_2, HONO); NO CL	>99.5% purity	1 L bath, 2 m reverse diffusion tube, heated stirring reactor
(Brust et al., 2000)	(R4)	FTIR (NO_2, HONO), IC (HONO)	up to 22ppm; <2% NO_2	20 cm reverse diffusion, heated reactor
(Schiller et al., 2001)	(R4)	TLDAS (HONO), FTIR (HONO) IC of KOH solutions	n/d	bubbled N_2 through 0.5 M HCl followed by reaction with solid sodium nitrite
(Perez et al., 2007)	(R4)	TD-CL, TD-LIF	observed ClNO	same setup as Febo et al. (1995)

(Perez et al., 2007)	(R2)	TD-CL, TD-LIF	>95%	flowed H_2SO_4 aerosol over $NaNO_2$ sandwiched between paper filters
(Roberts et al., 2010)	(R4)	IBBCEAS, NO_y-CL, CIMS	>95%	HCl gas cylinder (10 ppmv) and $NaNO_2$ reactor tube
(Ren et al., 2010)	(R4)	LOPAP, NO_y-CL, CIMS	n/d	Reverse diffusion tube, high [HCl] (9-12 M), tubing thickness not described
(Reed et al., 2016)	(R2)	Differential photolysis NO-CL; NO_2 CAPS; FTIR	HONO (70.4%; < 50 ppbv); NO (15%); NO_2 (12.8%); HNO_3 (1.3%)	Perm tube filled with 37% HCl placed in oven with $NaNO_2$ salt; flushed @ 1.5 slpm; <50 ppbv

415

Table 2. Summary of TD-CRDS analyses of the HONO source output. The RH of the diluent gas was in the range of 15% to 35%, except for experiments conducted with cylinder gases which are shown below the dashed line. The range of mixing ratios stated is for output after dilution. The stated errors are from regression analyses of plots of NO_2, NO_x or NO_x+ClNO vs. NO_y and are at the 1σ level. n/d = not determined.

Date	Setting	Diluent gas	Range (ppbv)	HONO (%)	NO_2 (%)	NO_x (%)	NO_x+ClNO (%)
Jan 16, 2019	Lab	Scrubbed air	0 - 140	*97.2±0.1	n/d	2.80±0.07	n/d
May 3, 2019	Lab	Scrubbed air	0 - 7	96.0±0.2	1.9±0.2	4.0±0.2	(4.0±0.2)**
May 6, 2019	Lab	Scrubbed air	0 - 93	96.4±0.4	1.9±0.4	3.6±0.4	(3.6±0.4)**
May 10, 2019	Lab	Scrubbed air	0 - 21	*97.6±0.1	1.10±0.03	2.40±0.05	n/d
May 17, 2019	Lab	Scrubbed air	0 - 38	98.7±0.1	0.01±0.02	0.92±0.01	1.25±0.01
May 22, 2019	Lab	Scrubbed air	0 - 14	97.7±0.1	1.29±0.06	1.54±0.06	2.28±0.04
Jan 17, 2020	Field	Scrubbed air	0 - 80	98.5±0.1	1.00±0.05	1.50±0.08	(1.50±0.08)**
Mar 19, 2020	Lab	Scrubbed air	0 - 320	*98.72±0.01	n/d	1.28±0.01	n/d
Jul 25, 2019	Lab	Cylinder O_2	0 - 95	86.60±0.02	4.60±0.03	n/d	13.4±0.02
Jan 30, 2020	Field	Cylinder N_2	0 - 50	81.3±0.1	5.90±0.09	n/d	18.7±0.1

* Upper limit. ** The TD-CRDS quartz inlet temperature was ramped between 300 °C and 600 °C; the TD-CRDS mixing ratios at an inlet temperature of 300 °C matched the NO_x mixing ratios observed with the room temperature inlet, indicating the absence of ClNO.